

DRAFT VERSION JANUARY 12, 2022

Typeset using L<sup>A</sup>T<sub>E</sub>X **preprint** style in AASTeX62

# Low- $\alpha$ Metal-Rich Stars with Sausage Kinematics in the LAMOST Survey: Are they from the Gaia-Sausage-Enceladus Galaxy?

GANG ZHAO\* AND YUQIN CHEN\*

## ABSTRACT

We search for metal-rich Sausage-kinematic (MRSK) stars with  $[\text{Fe}/\text{H}] > -0.8$  and  $-100 < V_\phi < 50 \text{ km/s}$  in LAMOST DR5 in order to investigate the influence of the Gaia-Sausage-Enceladus (GSE) merger event on the Galactic disk. For the first time, we find a group of low- $\alpha$  MRSK stars, and classify it as a metal-rich tail of the GSE galaxy based on the chemical and kinematical properties. This group has slightly larger  $R_{\text{apo}}$ ,  $Z_{\text{max}}$  and  $E_{\text{tot}}$  distributions than a previously-reported high- $\alpha$  group. Its low- $\alpha$  ratio does not allow for an origin resulting from the splash process of the GSE merger event, as is proposed to explain the high- $\alpha$  group. A hydrodynamical simulation by Amarante et al. provides a promising solution, in which the GSE galaxy is a clumpy Milky-Way analogue that develops a bimodal disk chemistry. This scenario explains the existence of MRSK stars with both high- $\alpha$  and low- $\alpha$  ratios found in this work. It is further supported by another new feature that a clump of MRSK stars is located at  $Z_{\text{max}} = 3 - 5 \text{ kpc}$ , which corresponds to the widely adopted disk-halo transition at  $|Z| \sim 4 \text{ kpc}$ . We suggest that a pile-up of MRSK stars at  $Z_{\text{max}}$  contributes significantly to this disk-halo transition, an interesting imprint left by the GSE merger event. These results also provide an important implication on the connection between the GSE and the Virgo Radial Merger.

*Keywords:* Galactic halo; Spiral arms and galactic disk; Chemical composition and chemical evolution; Kinematics, dynamics, and rotation

## 1. INTRODUCTION

It has building evidence that the Galaxy experienced several major merger events and left imprints on the stellar halo, in the forms of streams and overdensities in spatial position and/or clumps and groups in integrals of motion (e.g., energy, angular momenta, actions). Two famous mergers are the recent Sagittarius (Sgr) and the ancient Gaia-Sausage-Enceladus (GSE) dwarf galaxies. The former is witnessed by the existence of leading and trailing arms in a large sky coverage (Ibata et al. 1994), while the latter was discovered as the so-called ‘‘Gaia-Sausage’’ structure in the radial versus azimuthal velocity space (Belokurov et al. 2018; Myeong et al. 2018) without any dense stream detected so far. It is proposed that the GSE galaxy collided nearly head-on with the Galaxy and was

Corresponding author: Gang Zhao  
gzhao@nao.cas.cn

\* CAS Key Laboratory of Optical Astronomy, National Astronomical Observatories, Chinese Academy of Sciences, Beijing 100101, China

School of Astronomy and Space Science, University of Chinese Academy of Sciences, Beijing 100049, China

disrupted about 6 – 11 Gyr ago, leaving a giant cloud of intermediate-metallicity ( $[\text{Fe}/\text{H}] \sim -1.3$ ) stars on highly radial orbits (Helmi et al. 2018; Haywood et al. 2018; Fattahi et al. 2020). Tracing these events and searching for their imprints are our long-term goals in order to understand the building blocks of the Galactic halo, and perhaps also the Galactic disk, within the context of  $\Lambda$ CDM cosmology.

As a recent merger with the Galaxy at a relatively low inclination, the debris of Sgr are found all over the sky with Galactocentric distances ranging from 15 kpc to 130 kpc (Majewski et al. 2003; Belokurov et al. 2014; Sesar et al. 2017). Being on a high eccentricity orbit, the ancient GSE merger left its debris in a limited region on the sky within 20-30 kpc (Iorio & Belokurov, 2019), and delivered large amounts of stars into the solar neighborhood (Belokurov et al. 2018; Myeong et al. 2019). Interestingly, Gallart et al. (2019) suggested that low- $\alpha$  stars found by Nissen & Schuster (2010) within 0.3 kpc of the Sun are also debris of the GSE merger. The Sgr merger event provides a dominant component in the outer halo ( $R > 30$  kpc), while the accreted component in the inner halo (and the Solar neighborhood) mainly comes from the GSE merger (Naidu et al. 2020).

Meanwhile, Donlon et al. (2019) suggested that the GSE merger may be the same as the “Virgo Radial Merger (VRM),” which includes the Virgo Overdensity, the Virgo Stellar Stream, and many halo streams. They claimed that the Virgo Overdensity, the Hercules-Aquila Cloud and the Eridanus-Phoenix overdensity are probably unmixed portions of the GSE tidal debris. A systematic search for this connection has not been carried out and will become possible with the launch of the future 2-m Chinese Space Survey Telescope (CSST) project (Zhan et al. 2011) taking into account of its advantage of both deep field and high spatial resolution observations. Since stars belonging to the same structure share similar abundance patterns (Freeman et al. 2002), the chemical mapping of halo stars clustering in both spatial position and integrals of motion by the CSST project will open the door to reconstruct the Galactic past merging history.

Last but not least, it is proposed that the GSE merger event perturbed the proto-disk and produced a special metal-rich halo-like population in the biggest splash (Belokurov et al. 2019), which heats disk stars up to the Galactic halo. In support for this scenario, a low angular momentum ( $V_\phi < 100 \text{ km/s}$ ) stellar population with  $[\text{Fe}/\text{H}] > -1$  was found by Bonaca et al. (2017), and was classified as a “heated thick disk”, rather than an “in-situ halo.” Later, more works (Haywood et al. 2018; Di Matteo et al. 2019; Amarante et al. 2020a) reported the existence of Sausage-kinematic stars with thick-disk chemistry. They were named “splash” stars and become important imprints of the GSE merger event on the Galactic disk.

In this paper, we aim to search for additional imprints of the GSE merger event using the LAMOST low-resolution survey, in combination with Gaia DR2, based on the chemical and kinematical properties of disk-metallicity stars. Since the LAMOST survey provides the largest dataset of stars in the Galactic disk, it is favorable to investigate the influence of the GSE accretion event on the evolution of the Galactic disk. It is expected that more “splash” stars with disk chemistry can be found so that new merging imprints may be detected from a good statistic analysis on big data. Meanwhile, it is interesting to probe if there is a metal-rich tail of the GSE galaxy extending from the main component at  $[\text{Fe}/\text{H}] \sim -1.3$ , which will provide an important implication for its connection with the VRM because the Virgo Overdensity is metal rich and extends right into the Galactic disk.

## 2. SELECTION OF STAR SAMPLES

The first stage of the LAMOST spectroscopic survey (Zhao et al. 2006, 2012; Cui et al. 2012; Deng et al. 2012) was carried out in a low-resolution ( $R \sim 2000$ ) mode with a wide spectral wavelength coverage of  $3800 - 9000 \text{ \AA}$ . Based on abundances from APOGEE DR14 by Ting et al. (2019), Xiang et al. (2019) developed a data-driven neural network and derived stellar parameters and  $[\alpha/\text{Fe}]$  abundances for 8,162,566 stars from LAMOST DR5. This is an internally consistent dataset (hereafter DDPayne-LAMOST DR5) and thus becomes a good sample for a statistic study.

From this catalog, we select stars with  $[\text{Fe}/\text{H}] > -1.5$  and require the errors in both  $[\text{Fe}/\text{H}]$  and  $[\alpha/\text{Fe}]$  to be less than 0.1 dex. We divide the dataset into three samples according to the gravity range,  $2.6 < \log g < 3.3$  (LGB, low red-giant branch),  $2.2 < \log g < 2.6$  (RC, red clump) and  $0.0 < \log g < 2.2$  (UGB, upper red-giant branch). With this division, the analysis is based on more internally-consistent abundances within each sample than in the whole dataset by reducing the dependence of abundance on stellar parameters. Meanwhile, results from different samples can be compared and checked independently to draw a reliable conclusion. We do not include dwarf stars from DDPayne-LAMOST DR5 because their abundances are less reliable due to the uncertainty in the trained dataset of APOGEE DR14 (Zasowski et al. 2019).

APOGEE (Apache Point Observatory Galactic Evolution Experiment) (Majewski et al. 2017) is a medium-high resolution ( $R \sim 22,500$ ) spectroscopic survey in the near-infrared spectral range (H band,  $15700\text{--}17500 \text{ \AA}$ ). The most recent version is APOGEE DR16, which provides more reliable parameters and elemental abundances than APOGEE DR14 thanks to the updated pipeline ASPCAP (Garca Perez et al. 2016) using a grid of only MARCS stellar atmospheres (Gustafsson et al. 2008) and a new H-band line list (Smith et al. 2020).

We cross-match DDPayne-LAMOST DR5 with APOGEE DR16 and carry out calibrations of  $[\text{Fe}/\text{H}]$  and  $[\alpha/\text{Fe}]$  for the selected three samples. We limit stars with signal-to-noise larger than 80 and a good fitting quality of  $\chi_{\text{ASPCAP}} < 25$  from APOGEE DR16 to get reliable abundances for calibration. Fig. 1 shows the comparison of  $[\text{Fe}/\text{H}]$ ,  $[\alpha/\text{Fe}]$  and calibrations by linear fitting between the two datasets for the three samples. Corrections for  $[\text{Fe}/\text{H}]$  are applied to the three samples of DDPayne-LAMOST DR5 based on the individual calibration of each sample so that the results from DDPayne-LAMOST DR5 and APOGEE DR16 can be compared when necessary. We do not correct  $[\alpha/\text{Fe}]$  ratios because there are significant scatters in the calibrations, and we prefer to have internally consistent  $[\alpha/\text{Fe}]$  within each sample from DDPayne-LAMOST DR5 for separating the thin and thick disks in the following analysis.

We make use of distances from the StarHorse catalog for LAMOST DR5 by Queiroz et al. (2020) with the relative error in distance less than 10%. Radial velocities with errors less than  $10 \text{ km/s}$  are taken from LAMOST DR5 and proper motions with errors less than  $0.25 \text{ mas/yr}$  are from *Gaia* DR2 (Gaia Collaboration 2018). We check the quality of the *Gaia* astrometry with the renormalized unit weight error of  $RUWE < 1.44$  (Lindgren et al. 2018). Spatial velocities and orbital parameters are calculated based on the publicly available code *Galpot*. We employ the default potential of *MilkyWayPotential* provided by McMillan et al. (2017), the solar position of  $R = 8.2 \text{ kpc}$ , and the circular speed  $V_c = 233.1 \text{ km/s}$  (McMillan et al. 2011). The peculiar velocity of the Sun is  $(U_\odot, V_\odot, W_\odot) = (11.1, 12.24, 7.25) \text{ km/s}$  (Schonrich et al. 2010).

With abundances and velocities available, we select stars with  $-100 < V_\phi < 50 \text{ km/s}$  and  $[\text{Fe}/\text{H}] > -0.8$  as our targets based on the characteristics of the *Gaia*-Sausage structure, and we name them “metal-rich Sausage-kinematic (MRSK)” stars in this work. The choice of the upper limit of  $50 \text{ km/s}$

aims to avoid stars at  $V_\phi \sim 100 \text{ km/s}$ , which is the transition between the lower boundary of the thick disc and the upper boundary of the splash box (Belokurov et al. 2019). We adopt a lower limit of  $-100 \text{ km/s}$  in order to include more halo-kinematic disk-metallicity stars. This selection will not include stars from the Sequoia dwarf galaxy, which has retrograde orbits with  $V_\phi < -100 \text{ km/s}$  and is relatively metal poor with  $[\text{Fe}/\text{H}] < -1.5$  as shown in Belokurov et al. (2019).

Fig. 2 shows the  $V_R$  versus  $V_\phi$  diagrams and the contour maps of  $[\text{Fe}/\text{H}]$  versus  $[\alpha/\text{Fe}]$  for all stars with  $[\text{Fe}/\text{H}] > -0.8$  and  $R > 5 \text{ kpc}$  in the three samples. The latter limit is adopted to avoid stars from the bar/bulge region ( $R < 5 \text{ kpc}$ ). Within the two red lines, the existence of MRSK stars is obvious. For normal disk stars with  $[\text{Fe}/\text{H}] > -0.8$  and  $V_\phi > 150 \text{ km/s}$ , the separation between the high- $\alpha$  thick disk and the low- $\alpha$  thin disks is shown by the red line of  $[\alpha/\text{Fe}] = -0.08[\text{Fe}/\text{H}] + 0.12$  in the  $[\text{Fe}/\text{H}]$  versus  $[\alpha/\text{Fe}]$  diagram. This line will be adopted to pick out low- $\alpha$  MRSK stars from the high- $\alpha$  group in the following analysis. Here we try to adopt a strict criterion to select the low- $\alpha$  group by lowering the red line close to the boundary of the low- $\alpha$  contours for normal thin-disk stars.

### 3. TWO GROUPS OF MRSK STARS WITH HIGH- $\alpha$ AND LOW- $\alpha$ RATIOS

Fig. 3 shows the  $[\text{Fe}/\text{H}]$  versus  $[\alpha/\text{Fe}]$  diagrams for MRSK stars ( $-100 < V_\phi < 50 \text{ km/s}$  and  $[\text{Fe}/\text{H}] > -0.8$ ) in the three samples. The high- $\alpha$  group above the red line is expected to be the heated thick disk population, consisting of so-called “splash” stars, due to the massive merger event of the GSE galaxy as suggested by Belokurov et al. (2019). To our interest, a significant fraction of MRSK stars have low- $\alpha$  ratios, and they exist in three different samples. The low- $\alpha$  group extends to a higher metallicity of  $[\text{Fe}/\text{H}] \sim 0.0$  (or above) than the high- $\alpha$  group in each sample. The existence of low- $\alpha$  MRSK stars is not previously reported in the literature, and there are totally 1534 such stars in the three samples. We check that their Sausage-kinematic characteristics persists when we adopt the distance by inverting the parallax of *Gaia* DR2. It seems unlikely that errors in  $[\alpha/\text{Fe}]$  and/or kinematics can produce similar distributions in the  $[\text{Fe}/\text{H}]$  versus  $[\alpha/\text{Fe}]$  diagram for three different samples. Therefore, we suggest that this population of low- $\alpha$  MRSK stars is real.

As an independent check, we investigate if the low- $\alpha$  MRSK group exists in the APOGEE survey by applying the same procedure to APOGEE DR16 for stars in the gravity range of  $0 < \log g < 3.8$ . We adopt an extra criterion of  $DEC > -10 \text{ deg}$ , as similar as the sky coverage of the LAMOST survey, and with the purpose to avoid stars from Magellanic Clouds and Sagittarius Streams in the southern sky. Due to the small number of this population, we do not divide this dataset into three samples (LGB, RC and UGB) accordingly. As seen in Fig. 4, MRSK stars in APOGEE DR16 show both high- $\alpha$  and low- $\alpha$  ratios with an obvious gap, according to the same separation line as that of DDPayne-LAMOST DR5. The majority of MRSK stars belong to the high- $\alpha$  group, but the low- $\alpha$  group (consisting of 410 stars) is significant. Also, the low- $\alpha$  group in this sample has an similar extension toward super solar metallicity as in DDPayne-LAMOST DR5. If the systematic shift of 0.03 dex in  $[\alpha/\text{Fe}]$  to a lower value in APOGEE DR16 (see Fig. 1) is taken into account, the star number of the low- $\alpha$  group is slightly reduced (398 stars). In addition, the separation between the high- $\alpha$  and the low- $\alpha$  groups is more clear in APOGEE DR16 than in DDPayne-LAMOST DR5. Thus, the existence of a low- $\alpha$  MRSK group is significant and real in this independent dataset.

Finally, with close inspection on the data in Belokurov et al. (2019), we find that the  $[\text{Fe}/\text{H}]$  versus  $V_\phi$  trend in their Figure 2 also shows a hint on the existence of a metal-rich tail of the GSE galaxy. The distribution of stars with  $V_\phi \sim 0 \text{ km/s}$  seems to cross the splash box and extends to the metal-rich end until  $[\text{Fe}/\text{H}] \sim 0$ . Moreover, in the  $V_R$  versus  $V_\phi$  diagram as coded with  $[\alpha/\text{Fe}]$ ,

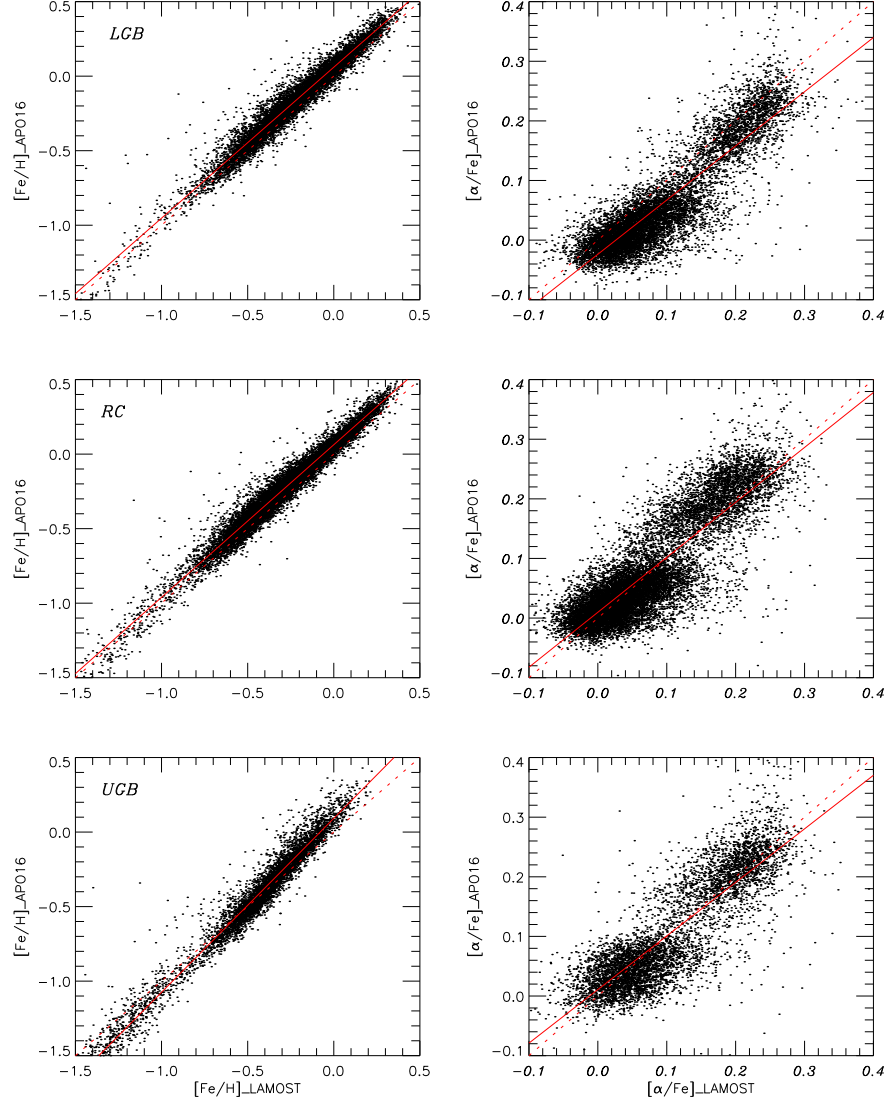


**Figure 1.** Comparison of  $[\text{Fe}/\text{H}]$  and  $[\alpha/\text{Fe}]$  between DDPayne-LAMOST DR5 and APOGEE DR16 for the three samples (LGB, RC and UGB). Red dash lines are the one-to-one relations and solid lines are calibrations derived from linear fits to the data.

Sausage-kinematic stars have both high- $\alpha$  and low- $\alpha$  ratios. This supports the reality of the low- $\alpha$  MRSK group.

#### 4. GALACTIC LOCATIONS AND ORBITAL PROPERTIES BETWEEN HIGH- $\alpha$ AND LOW- $\alpha$ MRSK STARS

##### 4.1. The $R$ , $|Z|$ , $R_{\text{apo}}$ and $Z_{\text{max}}$ distributions

The comparison of Galactic locations, in terms of  $R$  and  $|Z|$ , between the high- $\alpha$  and low- $\alpha$  groups for the three samples is shown in Fig. 5. The distributions of the high- $\alpha$  group are reduced by a factor of three in order to have similar peaks as the low- $\alpha$  group for comparison. Generally, there is no obvious difference in both  $R$  and  $|Z|$  distributions between the high- $\alpha$  and low- $\alpha$  groups for the LGB and the RC samples. As the luminosity increases (and includes more distant stars) from the



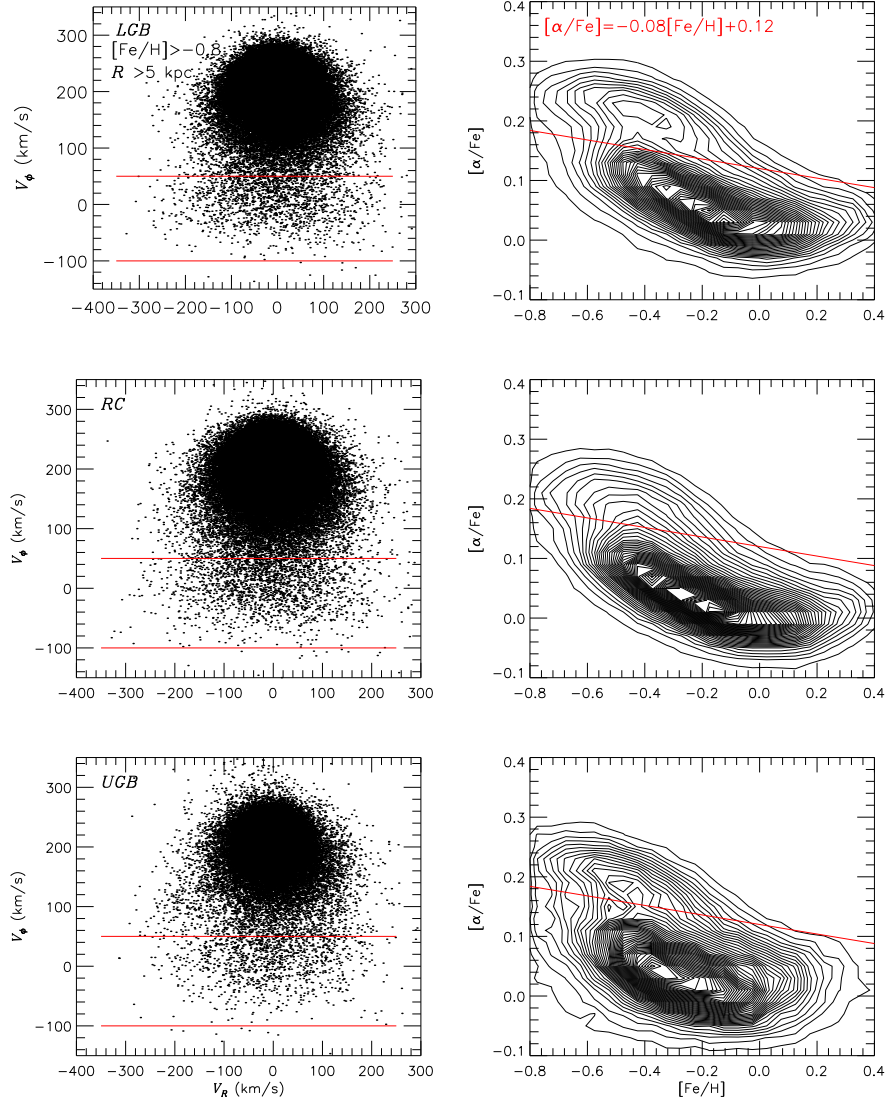


**Figure 2.** Left:  $V_R$  versus  $V_\phi$  diagram for stars with  $[\text{Fe}/\text{H}] > -0.8$  and  $R > 5$  kpc in the three samples. The two red lines show the definition of metal-rich Sausage-kinematic (MRSK) stars within  $-100 < V_\phi < 50$  km/s. Right: Contour maps of  $[\text{Fe}/\text{H}]$  versus  $[\alpha/\text{Fe}]$  for the three samples. Red lines are defined to separate between the thin and thick disks, which will be used to pick out the low- $\alpha$  group from the high- $\alpha$  group among MRSK stars.

LGB/RC to UGB samples, we would expect to observe more old high- $\alpha$  stars than young low- $\alpha$  stars in the UGB sample. However, this is not the case and we observe an opposite trend for the UGB sample. If the low- $\alpha$  group belongs to the locally-born thin-disk population, it would be located below the splashed high- $\alpha$  thick disk. Moreover, the GSE merger event happened about 9 Gyr ago, before the formation of the thin disk. Thus, it is unlikely that these low- $\alpha$  MRSK stars belong to the young thin-disk population, and were splashed up to the halo during the GSE merger event. We suggest that its low- $\alpha$  ratio indicates an origin from the accreted halo (i.e. the GSE galaxy itself), rather than from the thin disk.

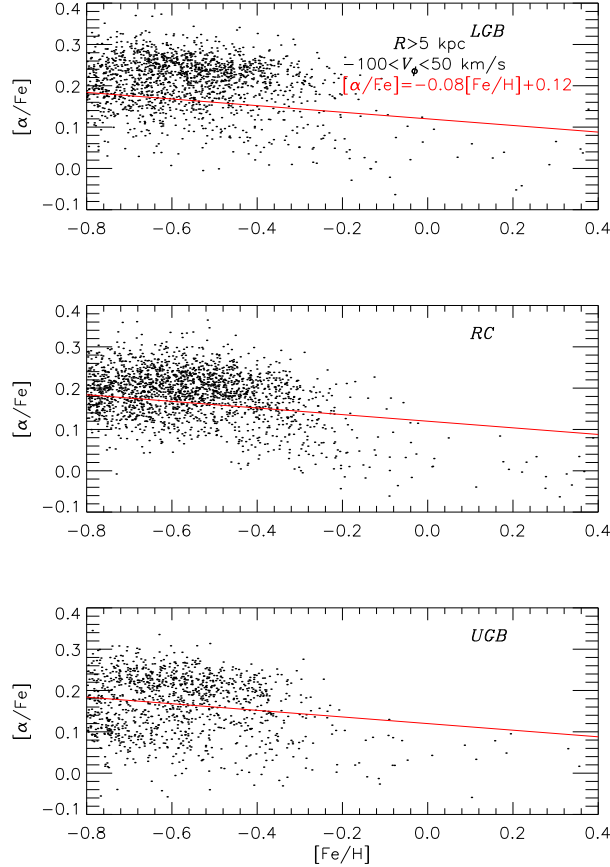


**Figure 3.**  $[\text{Fe}/\text{H}]$  versus  $[\alpha/\text{Fe}]$  diagrams for the three samples in DDPayne-LAMOST DR5 data. The red lines are the same as in Fig. 2.

It is interesting to investigate how far the accreted low- $\alpha$  group would go in the Galaxy and how different in the maximum distance as compared with the splashed high- $\alpha$  group. In Fig. 6, the histograms of  $R_{\text{apo}}$  and  $Z_{\text{max}}$  are shown for both groups in the three samples. Obviously, the low- $\alpha$  group shows a systematic shift toward a larger  $R_{\text{apo}}$  by 1 – 2 kpc. Specifically, the LGB sample shows a peak at 8.5 kpc for the high- $\alpha$  group and at 10.5 kpc for the low- $\alpha$  group despite of their similar  $R$  and  $|Z|$  distributions. The  $R_{\text{apo}}$  distributions of the low- $\alpha$  group have wide peaks around 10 kpc for RC and UGB samples, extending up to 15 kpc. The  $Z_{\text{max}}$  distributions generally have peaks around 4 kpc for both groups but the low- $\alpha$  group has extensions toward higher values in the three samples. These distributions show that the low- $\alpha$  group is not from the thin disk, which can not reach a vertical distance as high as the typical thick disk and would lie far below the splashed thick disk. Finally, in view of the head-on collision of the GSE galaxy with the Galaxy, similar peaks at 4 kpc in the  $Z_{\text{max}}$  distributions between the low- $\alpha$  and high- $\alpha$  groups may suggest that they are related, and probably are connected by the same event. We will discuss this possibility later.

#### 4.2. The $R_{\text{m}} - Z_{\text{max}}$ and $e - Z_{\text{max}}$ planes

As compared with its present location  $R$ , the mean Galactic distance  $R_{\text{m}}$ , as defined to be  $(R_{\text{apo}} + R_{\text{peri}})/2.0$ , provides more information on a star's origin. Fig. 7 shows the  $R_{\text{m}}$  versus  $Z_{\text{max}}$  and the  $e$  versus  $Z_{\text{max}}$  planes for MRSK stars. Interestingly, there are three sections for both the high-

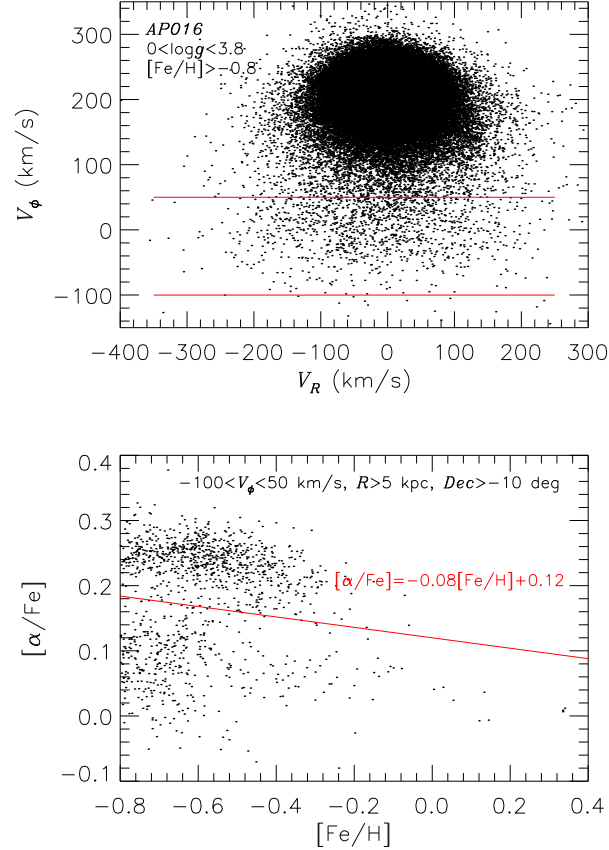


**Figure 4.** Upper:  $V_R$  versus  $V_\phi$  (upper) diagram for stars with  $0.0 < \log g < 3.8$ ,  $[\text{Fe}/\text{H}] > -0.8$  and  $Dec > -10$  in APOGEE DR16. Lower: Contour map of  $[\text{Fe}/\text{H}]$  versus  $[\alpha/\text{Fe}]$  for MRSK stars (with  $[\text{Fe}/\text{H}] > -0.8$  and  $-100 < V_\phi < 50 \text{ km/s}$ ) in APOGEE DR16. Lines are the same as in Fig. 2.

$\alpha$  (small dots) and low- $\alpha$  groups. In particular, there is a clear gap along the black solid line of  $Z_{\text{max}} = 0.26R_{\text{m}} + 0.4$ . We note that, normal disk stars with  $V_\phi > 150 \text{ km/s}$  are all located in the lowest panel of  $Z_{\text{max}} < 2 \text{ kpc}$ . That is, stars from the thin-disk population has  $Z_{\text{max}} < 2 \text{ kpc}$  and never show up at  $|Z| > 2 \text{ kpc}$ . This is a further support for the suggestion that the low- $\alpha$  MRSK group does not belong to the thin disk population. Most MRSK stars from the low- $\alpha$  group occupy the upper two sections with only a few exceptions. The upper two sections are further separated by the dash line of  $Z_{\text{max}} = 0.9R_{\text{m}} + 1.4$ , with blue open circles for the middle sections and red circles for the upper sections. The division lines are arbitrarily drawn by eye to separate the three sections, and we compare the results within each section. These features share similar characteristics to those in the  $R_{\text{apo}} - Z_{\text{max}}$  diagram of [Amarante et al. \(2020b\)](#), which are caused by resonant trapping effects of the Galactic bar ([Moreno et al. 2015](#)). Interestingly, [Schuster et al. \(2019\)](#) had shown that 3D star orbits of the high- $\alpha$  star G18-39 and the low- $\alpha$  star G21-22 in [Nissen & Schuster \(2010\)](#) are trapped by 2D resonant families V and IX of [Moreno et al. \(2015\)](#). Different orbital families in [Moreno et al. \(2015\)](#) would reach different  $Z_{\text{max}}$ , which explains the appearance of the three sections in Fig. 7.

The distribution of MRSK stars in three sections was previously reported by [Haywood et al. \(2018\)](#) in the  $RD_{\text{max}}$  versus  $Z_{\text{max}}$  diagram (their Fig. 8) for the high- $\alpha$  group. In this work, we found similar



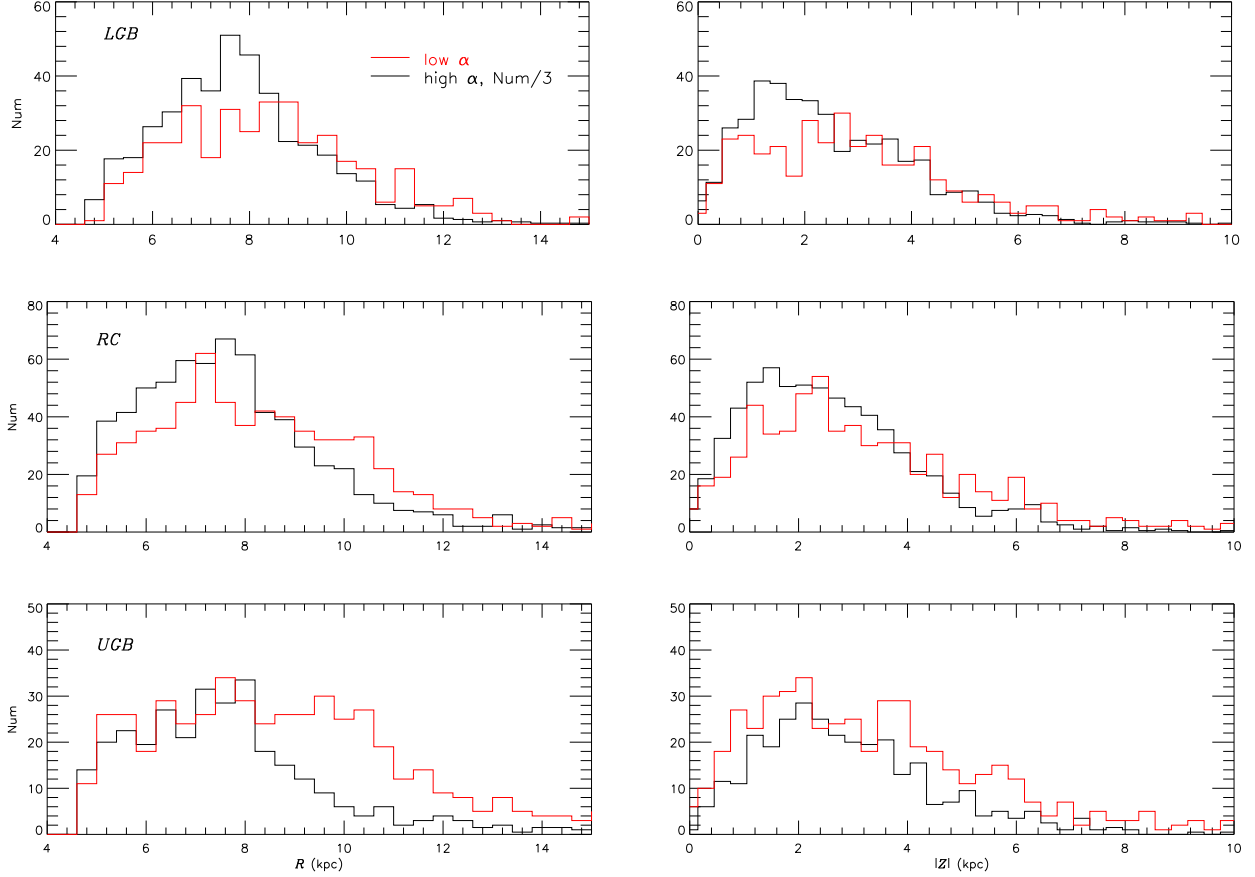


**Figure 5.** Histograms of  $R$  (left) and  $|Z|$  (right) for MRSK stars with high- $\alpha$  (black) and low- $\alpha$  (red) ratios in the three samples of DDPayne-LAMOST DR5.

three-section distributions for the low- $\alpha$  group in the  $R_m$  versus  $Z_{\max}$  diagram. This feature is unique to the GSE merger as a result from its high eccentricity of  $e > 0.7$ . As we limit stars with  $e > 0.9$ , five sections appear, while stars with  $e < 0.2$  show only one section at the lowest part of  $Z_{\max} < 2$  kpc. In view of this dependence, we show the  $e$  versus  $Z_{\max}$  diagrams for stars in the three sections on the right panels of Fig. 7. Interestingly, stars in the middle sections show a clump at  $Z_{\max} = 3 - 5$  kpc along the blue line of  $Z_{\max} = 8.5e - 3.5$ , while the upper sections show sparse distributions without any clump. There are 82%, 64% and 66% stars in the middle sections located within 1 kpc (two blue dash lines) along the solid blue lines for the three samples.

We investigate the distribution of the vertical velocity  $V_z$  for stars within two blue dash lines. There is almost zero  $V_z$  with a small dispersion of  $45 \text{ km/s}$ , significantly lower than that of  $\sim 90 \text{ km/s}$  for stars above the upper blue dashed line and of  $\sim 110 \text{ km/s}$  for the Galactic halo. In particular, the  $V_z$  dispersion of  $45 \text{ km/s}$  is typical for the thick disk. Therefore, these clump stars from the accreted halo could be regarded as the thick disk in kinematics. We thus propose a scenario that a pile-up of stars at  $Z_{\max} = 3 - 5$  kpc by the GSE merger event contributes significantly to (or may be responsible for) the division between the thick disk and the halo at  $|Z| \sim 4$  kpc, widely adopted in the literature (Kinman et al. 2011; Fernandez-Alvar et al. 2019). In this scenario, due to the negligible velocity in both  $V_\phi$  and  $V_z$ , these clump stars, with either low- $\alpha$  or high- $\alpha$  ratio, will stay

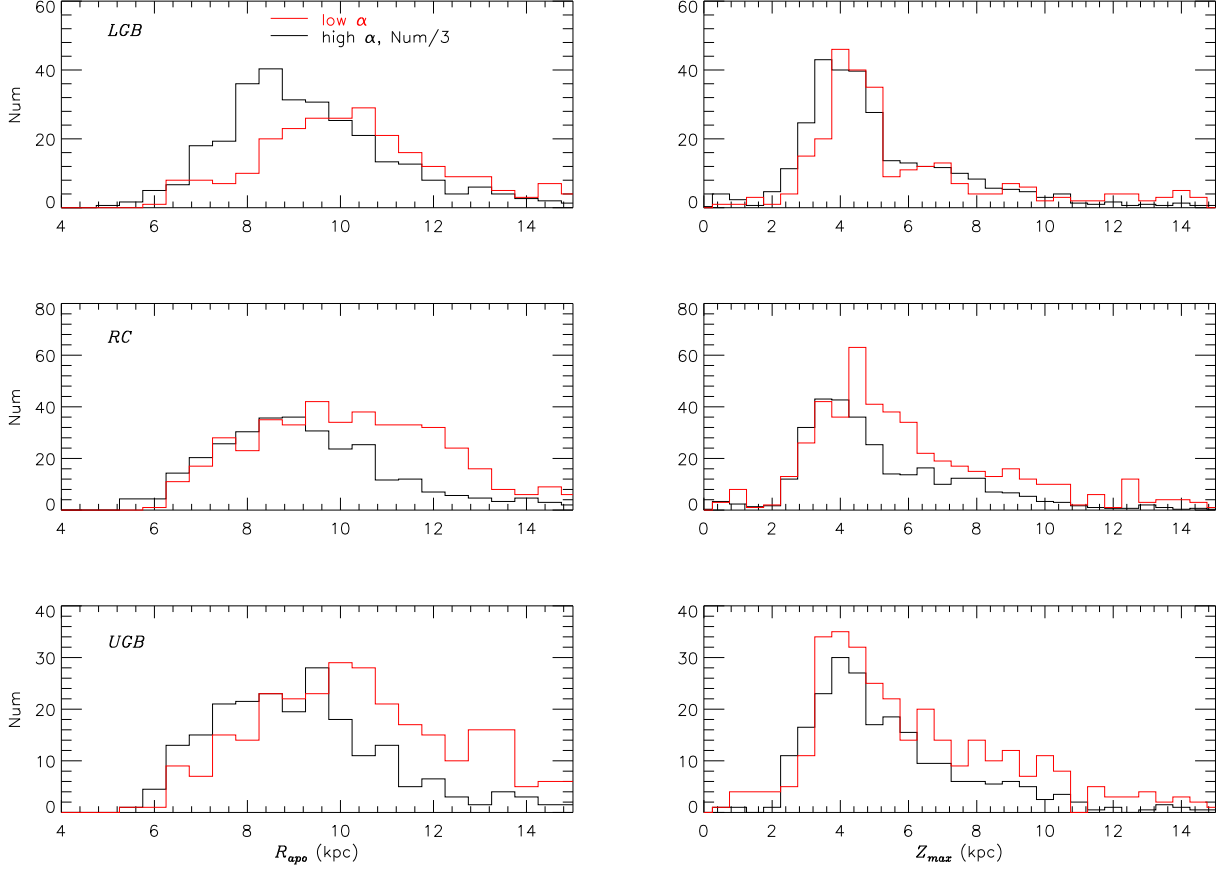


**Figure 6.** Histograms of  $R_{\text{apo}}$  (left) and  $Z_{\text{max}}$  (right) for MRSK stars with high- $\alpha$  (black) and low- $\alpha$  (red) ratios in the three samples of DDPayne-LAMOST DR5.

at the maximum vertical distance ( $Z_{\text{max}}$ ) for a longer time than in other positions, which leads to a pile-up of stars at this distance. Specifically, the pile-up at  $Z_{\text{max}} = 3 - 5$  kpc (due to the GSE merger event) produces an observational feature that there is a high density of stars at  $|Z| \sim 4$  kpc, beyond which the star number decreases. Thus this clump is regarded as the division between the thick disk and the halo. This suggestion is inspired by [Deason et al. \(2013\)](#) who proposed that a rapid transition in structural properties of the Galactic stellar halo at the break radius of 20-30 kpc ([Watkins et al. 2009](#); [Deason et al. 2011](#)) is due to the pile-up in  $R_{\text{apo}}$  of the tidal debris from a small number of significant mergers, e.g. the Sgr galaxy. Note that the intermediate-eccentricity orbit of the Sgr merger event will lead to the pile-up of stars in  $R_{\text{apo}}$ . With high-eccentricity stars, the GSE head-on merger event tends to cause a pile-up in  $Z_{\text{max}}$ , rather than  $R_{\text{apo}}$ . It is important to point out that both the low- $\alpha$  and high- $\alpha$  groups contribute to the formation of the high density of stars at  $|Z| \sim 4$  kpc, and thus they could be related to the same merger event. This suggestion is also consistent with the result by [Helmi et al. \(2018\)](#) that the GSE merger led to the formation of the Galactic inner halo and the thick disk.

#### 4.3. The $L_z$ versus $E_{\text{tot}}$ diagram

Fig. 8 shows the  $L_z$  versus  $E_{\text{tot}}$  diagrams for the low- $\alpha$  group in the three sections, as well as the the high- $\alpha$  group (small dots). With significant overlapping, the lowest section lies both sides, and

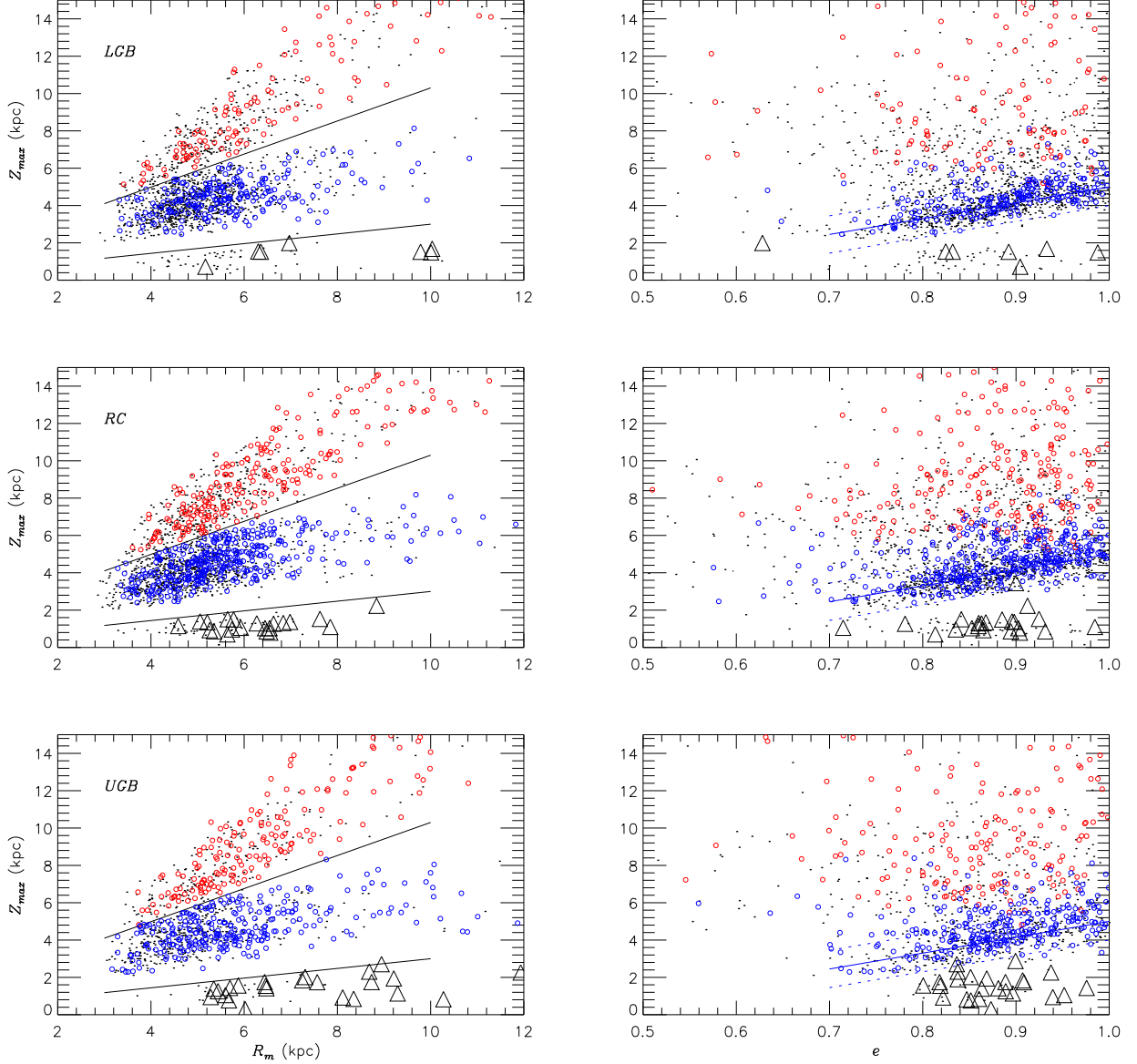


**Figure 7.**  $R_m$  versus  $Z_{\max}$  (left) and  $e$  versus  $Z_{\max}$  (right) diagrams for MRSK stars with high- $\alpha$  (black dots) and low- $\alpha$  (others) ratios in the three samples of DDPayne-LAMOST DR5. Low- $\alpha$  MRSK stars in the three sections are shown by black triangles (lowest), blue circles (middle) and red circles (upper).

the upper section distributes more close to the central part around  $L_z \sim 0$  and has a higher energy than the middle section. Specifically, the lowest parts of Fig. 8 are occupied by stars in the middle sections (blue circles) and the highest parts are mainly stars from the upper sections (red circles). However, the overlapping of both groups is dominated at  $E_{\text{tot}}/10^5 \sim -1.7 \text{ km}^2 \text{ s}^{-2}$ . Therefore, we favor for the suggestion that no obvious difference between the low- $\alpha$  and high- $\alpha$  groups is found in this diagram.

The energy of MRSK stars is above the low boundary of the GSE galaxy at  $E_{\text{tot}}/10^5 \sim -1.9 \text{ km}^2 \text{ s}^{-2}$ , although its metal poor component lies at  $E_{\text{tot}}/10^5 \sim -1.5 \text{ km}^2 \text{ s}^{-2}$  according to [Horta et al. \(2020\)](#). In addition, the energy of the GSE galaxy is significantly lower than the Sgr galaxy at  $E_{\text{tot}}/10^5 \sim$

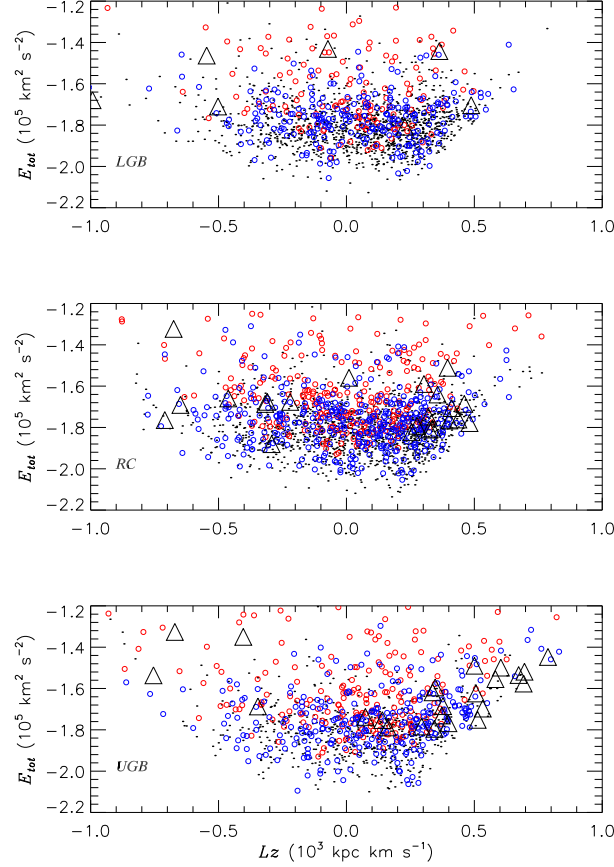


**Figure 8.**  $L_z$  versus  $E_{\text{tot}}$  diagrams for MRSK stars with high- $\alpha$  (black) and low- $\alpha$  (red) ratios in the three samples of DDPayne-LAMOST DR5. Symbols are the same as in Fig. 7.

$-1.0 \text{ km}^2 \text{ s}^{-2}$  according to [Naidu et al. \(2020\)](#) (see their Fig. 23). Due to its higher energy, the Sgr merger event has significant influence on the Galactic halo, since the majority of member stars can reach up to the outer Galaxy (beyond  $20 - 30 \text{ kpc}$ ). The lower energy of the GSE merger event makes it contribute significantly to the formation of the Galactic disk, for example, producing a clump of stars at  $Z_{\text{max}} = 3 - 5 \text{ kpc}$ .

## 5. THE ORIGIN OF THE LOW- $\alpha$ MRSK GROUP

### 5.1. Connecting the low- $\alpha$ group to the GSE galaxy

It is well known that Magellanic Clouds (MCs) and Sgr streams have metal rich components. In APOGEE DR16, it is possible to compare the low- $\alpha$  MRSK stars with member stars from MCs and Sgr in the  $[\text{Fe}/\text{H}]$  versus  $[\alpha/\text{Fe}]$  diagram. For this purpose, stars with “programnames” of “magclouds” and “Sgr” in APOGEE DR16 are picked out, and we limit stars within the range of  $-100 < V_\phi < 50 \text{ km/s}$ , i.e. Sausage-kinematics. In Fig. 9, these low- $\alpha$  MRSK stars (red circles) are compared with Sausage kinematic stars from MCs (green crosses) and Sgr (blue squares), as well as the metal poor GSE members (black dots). It shows that the low- $\alpha$  MRSK group is distinct from MCs at  $[\text{Fe}/\text{H}] < -0.8$ , but has some overlapping at  $-0.8 < [\text{Fe}/\text{H}] < -0.4$ . Meanwhile, GSE has higher  $[\alpha/\text{Fe}]$  than Sgr for the whole metallicity range of  $-1.4 < [\text{Fe}/\text{H}] < -0.2$ , and thus the low- $\alpha$  MRSK group does not belong to the Sgr galaxy. In short, the low- $\alpha$  MRSK stars in APOGEE DR16

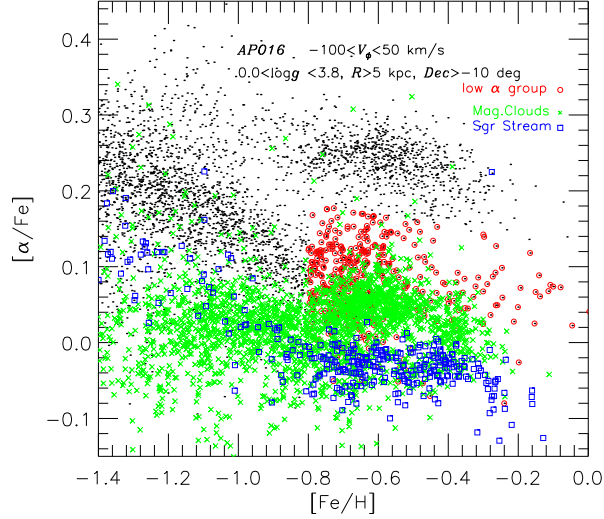


**Figure 9.**  $[\text{Fe}/\text{H}]$  versus  $[\alpha/\text{Fe}]$  diagrams for Sausage-kinematic stars with  $[\text{Fe}/\text{H}] > -1.5$ ,  $R > 5$  kpc and  $\text{Dec} > -10$  in APOGEE DR16. Sausage-kinematic stars from Magellanic Clouds (green crosses) and Sagittarius streams (blue squares) are overplotted.

are distinct from the member stars of MCs and Sgr. They belong to the GSE galaxy as addressed in Sect. 4.1.

In Fig. 10, stars with  $[\text{Fe}/\text{H}] > -1.5$  and  $-100 < V_\phi < 50 \text{ km/s}$  in DDPayne-LAMOST DR5 data are shown in the  $[\text{Fe}/\text{H}]$  versus  $[\alpha/\text{Fe}]$  diagrams with the same symbols and colors for the three sections as in Fig. 7. Three features in Fig. 10 are interesting and useful for understanding the origin of the low- $\alpha$  group. Firstly, there is no difference in  $[\alpha/\text{Fe}]$  among the three sections for the low- $\alpha$  group. All of them belong to the same population. Secondly, the contour maps show the main component of the GSE galaxy at  $[\text{Fe}/\text{H}] \sim -1.3$  and the second component at  $[\text{Fe}/\text{H}] \sim -0.5$  with a low-density gap at  $[\text{Fe}/\text{H}] \sim -0.8$ . Thirdly, the second component becomes weaker from the LGB, through the RC, to the UGB samples, as the weak low- $\alpha$  tail becomes more significant. In the UGB sample, there is a clear trend of  $[\alpha/\text{Fe}] = -0.20[\text{Fe}/\text{H}] - 0.05$  that connects the low- $\alpha$  MRSK group with the main GSE component at  $[\text{Fe}/\text{H}] \sim -1.3$ . This connection provides a strong support for the suggestion that the low- $\alpha$  MRSK group in DDPayne-LAMOST DR5 is the metal-rich tail of the GSE galaxy. By shifting the red line upward by 0.05 dex, the trend of  $[\alpha/\text{Fe}] = -0.20[\text{Fe}/\text{H}]$  indicates the existence of the metal-rich tail of the GSE galaxy in the LGB and RC samples.

### 5.2. A scenario for the origin of the low- $\alpha$ MRSK group

As described in Sect. 4, similar properties of the low- $\alpha$  and high- $\alpha$  MRSK groups in the  $R_m$ - $Z_{\text{max}}$  and  $e$ - $Z_{\text{max}}$  diagrams indicate that they probably result from the same process. However, the proposed splash process by the GSE merger event for the origin of the high- $\alpha$  group by Belokurov et al. (2019) can not explain the existence of the low- $\alpha$  group. Since  $\alpha$  is an age-sensitive abundance (Delgado et al. 2019), the low- $\alpha$  ratio of this MRSK group indicates a young population, which is not compatible with the splash process of the GSE merger event happened at an ancient time.

Without a splash process, Amarante et al. (2020a) developed a hydrodynamical simulation, in which a clumpy Milky-Way-like analogue succeeds to produce a bimodal disk chemistry with Sausage-



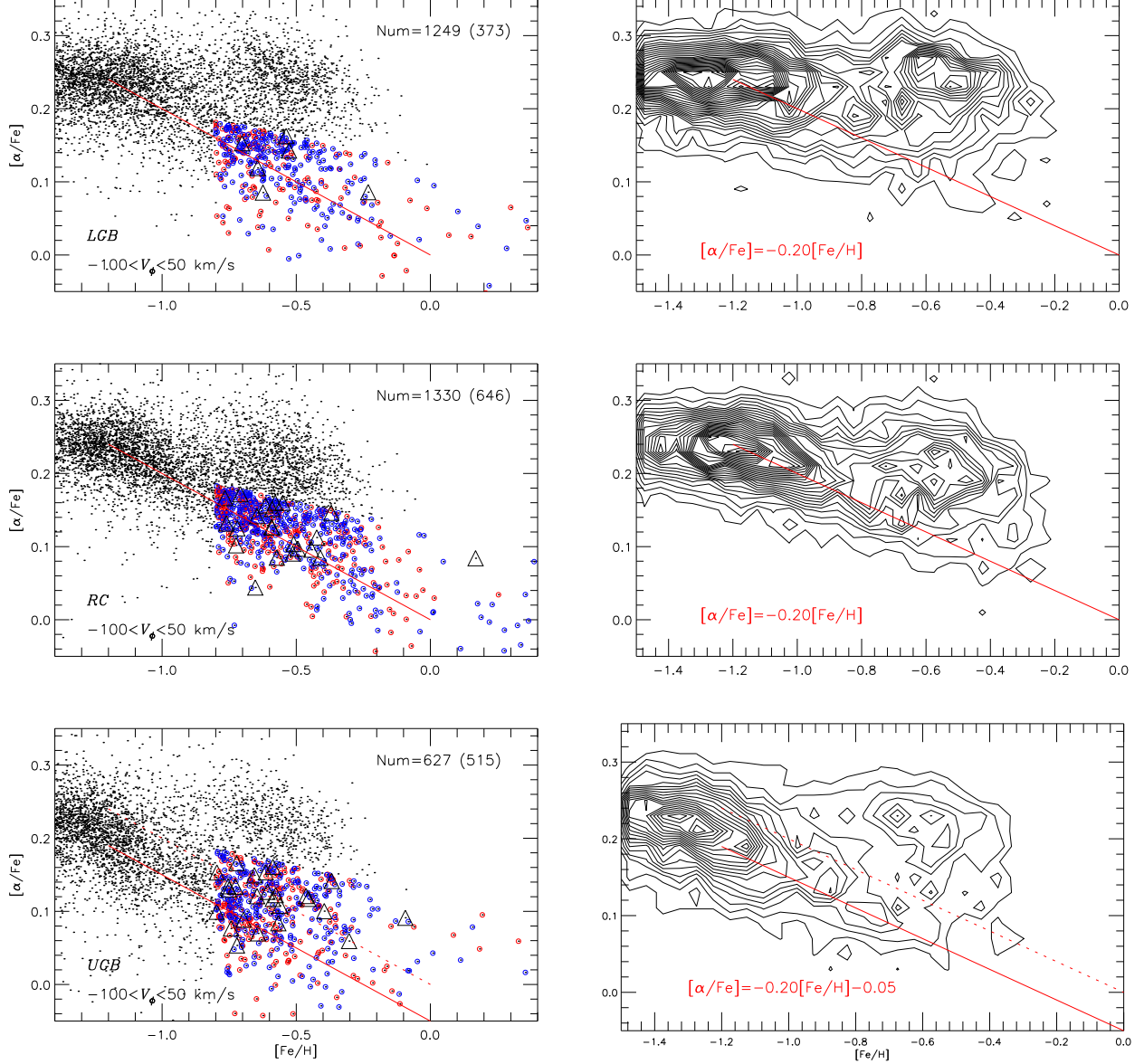


**Figure 10.**  $[\text{Fe}/\text{H}]$  versus  $[\alpha/\text{Fe}]$  diagrams and their contour maps for Sausage-kinematic stars with  $[\text{Fe}/\text{H}] > -1.5$  and  $R > 5$  kpc in the three samples of DDPayne-LAMOST DR5. Symbols are the same as in Fig. 7.

kinematics, similar as our data. In their Fig. 1, stars with  $-100 < V_\phi < 50 \text{ km/s}$  have metallicity range from  $[\text{Fe}/\text{H}] = -1.5$  to solar metallicity. Moreover, both high- $\alpha$  and low- $\alpha$  stars exist in the disk metallicity range of  $[\text{Fe}/\text{H}] > -0.8$  (their Fig. 2). In particular, this scenario does not need to exclude the GSE merger event. According to Mandelker et al. (2014), clumps in a galaxy can have an ex-situ origin associated to mergers. It is possible that the GSE merger event had brought the gas-rich cloud into the Galaxy at an early time, and produced clumps that developed the bimodal chemistry such as the high- $\alpha$  and low- $\alpha$  MRSK stars in later evolution. This is a promising solution to the existence of low- $\alpha$  MRSK stars, but it requires further study to fit into the case of the GSE dwarf galaxy in more details.

## 6. SUMMARY AND CONCLUSIONS

A large sample of stars with disk metallicity in the LAMOST survey provides us a good opportunity to find additional imprints of the GSE merger event and to extend the search for its member stars toward solar metallicity. With this purpose, metal-rich stars with Sausage-kinematics, i.e.  $[\text{Fe}/\text{H}] > -0.8$  and  $-100 < V_\phi < 50 \text{ km/s}$ , in LAMOST DR5 are analyzed in spatial, chemical and kinematical planes. We divide the stars into three samples (LGB, RC and UGB) so that our analysis is based on higher internally-consistent abundances within each sample of the low-resolution LAMOST survey.

A group of low- $\alpha$  MRSK stars is found, and it is thought to be the metal-rich component of the GSE merger. In the UGB sample, there is a continuous trend of  $[\alpha/\text{Fe}] = -0.20[\text{Fe}/\text{H}] - 0.05$  that connects it to the main body of the GSE galaxy at  $1.3 < [\text{Fe}/\text{H}] < -1.1$ . Moreover, it has larger  $R_{\text{apo}}$  (and  $Z_{\text{max}}$ ) distributions than those of high- $\alpha$  MRSK stars, which excludes the possibility to be the low- $\alpha$  thin disk population. This is the first report on the existence of a metal-rich tail of the GSE galaxy taking advantage of the large number of disk-metallicity stars in the LAMOST survey. It provides important implication on the connection between the GSE galaxy and the Virgo Radial Merger.

In the  $R_{\text{m}}$  versus  $Z_{\text{max}}$  plane, both the high- $\alpha$  and low- $\alpha$  groups show three-section distributions separated by  $Z_{\text{max}} = 0.26R_{\text{m}} + 0.4$  and  $Z_{\text{max}} = 0.90R_{\text{m}} + 1.0$  lines. This feature is unique to the GSE galaxy due to its high eccentricity of  $e > 0.7$ . Most MRSK stars are located in the middle and upper sections, while disk-metallicity stars with  $V_\phi > 150 \text{ km/s}$  limit within the lowest section of  $Z_{\text{max}} < 2$  kpc. According to [Amarante et al. \(2020b\)](#), the three-section distributions in the  $R_{\text{m}}$  versus  $Z_{\text{max}}$  plane are caused by different orbital families presented in [Moreno et al. \(2015\)](#).

We find an interesting clump of MRSK stars at  $Z_{\text{max}} = 3 - 5$  kpc, along the line of  $Z_{\text{max}} = 8.5e - 3.5$  in the  $e$  versus  $Z_{\text{max}}$  diagrams. Since this clump has negligible velocity in  $V_\phi$  and  $V_z$ , its stars would spend a longer time at  $Z_{\text{max}}$  than in other positions, leading to a pile-up of MRSK stars at  $|Z| = 3 - 5$  kpc. This clump corresponds to the widely-adopted disk-halo transition at  $|Z| \sim 4$  kpc, and thus is an interesting imprint left by the GSE merger event. This is new evidence for the scenario by [Helmi et al. \(2018\)](#) that the GSE merger event led to the formation of the Galactic inner halo and the thick disk.

The splash process of the GSE merger event, as proposed to explain the high- $\alpha$  MRSK group, fails to account for the low- $\alpha$  group because the ancient GSE merger event happened before its formation. Instead, a clumpy Milky-Way-like analogue in the hydrodynamical simulation by [Amarante et al. \(2020a\)](#) can produce a bimodal disk chemistry, similar as our data, without the need for a splash process. Based on this scenario, both high- $\alpha$  and low- $\alpha$  MRSK stars in the LAMOST survey belong to the GSE galaxy. The ancient GSE merger event had brought the gas-rich cloud into the Galaxy at an early time, and produced clumps that developed this bimodal chemistry for MRSK stars in later evolution. This is a promising solution to the origin of the low- $\alpha$  MRSK stars, but further study using simulations is necessary to confirm this scenario.

## ACKNOWLEDGEMENTS

This study is supported by the National Natural Science Foundation of China (Grant Nos. 11988101, 11625313, 11890694), National Key R&D Program of China (Grant No. 2019YFA0405502) and the 2-m Chinese Space Survey Telescope project. We would like to extend our sincere thanks to Dr. Sarah A. Bird for her kind help.

Guoshoujing Telescope (the Large Sky Area Multi-Object Fiber Spectroscopic Telescope, LAMOST) is a National Major Scientific Project has been provided by the National Development and Reform Commission. LAMOST is operated and managed by the National Astronomical Observatories, Chinese Academy of Sciences.

Funding for the Sloan Digital Sky Survey IV has been provided by the Alfred P. Sloan Foundation, the U.S. Department of Energy Office of Science, and the Participating Institutions. SDSS-IV acknowledges support and resources from the Center for High-Performance Computing at the University of Utah. The SDSS web site is [www.sdss.org](http://www.sdss.org).

SDSS-IV is managed by the Astrophysical Research Consortium for the Participating Institutions of the SDSS Collaboration including the Brazilian Participation Group, the Carnegie Institution for Science, Carnegie Mellon University, the Chilean Participation Group, the French Participation Group, Harvard-Smithsonian Center for Astrophysics, Instituto de Astrofísica de Canarias, The Johns Hopkins University, Kavli Institute for the Physics and Mathematics of the Universe (IPMU) / University of Tokyo, the Korean Participation Group, Lawrence Berkeley National Laboratory, Leibniz Institut für Astrophysik Potsdam (AIP), Max-Planck-Institut für Astronomie (MPIA Heidelberg), Max-Planck-Institut für Astrophysik (MPA Garching), Max-Planck-Institut für Extraterrestrische Physik (MPE), National Astronomical Observatories of China, New Mexico State University, New York University, University of Notre Dame, Observatorio Nacional/ MCTI, The Ohio State University, Pennsylvania State University, Shanghai Astronomical Observatory, United Kingdom Participation Group, Universidad Nacional Autónoma de México, University of Arizona, University of Colorado Boulder, University of Oxford, University of Portsmouth, University of Utah, University of Virginia, University of Washington, University of Wisconsin, Vanderbilt University, and Yale University.

## REFERENCES

- J.A.S. Amarante, L. Beraldo e Silva, V.P. Debattista, M.C. Smith, *ApJ*, 891, L30 (2020)
- J.A.S. Amarante, M.C. Smith, and C. Boeche, *MNRAS*, 492, 3816 (2020)
- A. Bonaca, C. Conroy, A. Wetzel, P.F. Hopkins, and D. Keres, *ApJ*, 845, 101 (2017)
- V. Belokurov, S.E. Koposov, N.W. Evans et al., *MNRAS*, 437, 116 (2014)
- V. Belokurov, D. Erkal, N.W. Evans, S.E. Koposov, and A.J. Deason, *MNRAS*, 478, 611 (2018)
- V. Belokurov, J.L. Sanders, A. Fattahi et al., *MNRAS*, 494, 3880 (2020)
- X.-Q. Cui, Y.-H. Zhao, Y.-Q. Chu et al., *Research in Astronomy and Astrophysics*, 12, 735 (2012)
- L.-C. Deng, H.J. Newberg, C. Liu et al., *Research in Astronomy and Astrophysics*, 12, 1197 (2012)
- A.J. Deason, V. Belokurov, N.W. Evans, and K.V. Johnston, *ApJ*, 763, 113 (2013)
- A.J. Deason, V. Belokurov, and N.W. Evans, *MNRAS*, 416, 2903 (2011)
- P. Di Matteo, M. Haywood, M.D. Lehnert et al., *A&A*, 632, A4 (2019)
- T.I. Donlon, H.J. Newberg, J. Weiss, P. Amy, and J. Thompson, *ApJ*, 886, 76 (2019)
- E. Delgado Mena, A. Moya, V. Adibekyan, et al. *A&A*, 624, 78 (2019)
- A. Fattahi, A.J. Deason, C.S. Frenk et al., *MNRAS*, 497, 4459 (2020)
- E. Fernandez-Alvar, J.G. Fernandez-Trincado, E. Moreno et al., *MNRAS*, 487, 1462 (2019)
- K. Freeman, and J.Bland-Hawthorn, *ARA&A*, 40, 487 (2002)
- Gaia Collaboration, C. Babusiaux, F. van Leeuwen et al., *A&A*, 616, A10 (2018)
- A.E. Garca Perez, C. Allende Prieto, J.A. Holtzman et al., *AJ*, 151, 144 (2016)
- C. Gallart, E.J. Bernard, C.B. Brook et al., *Nature Astronomy*, 3, 932 (2019)
- B. Gustafsson, B. Edvardsson, K. Eriksson et al., *A&A*, 486, 951 (2008)

- M. Haywood, P. Di Matteo, M.D. Lehnert et al., *ApJ*, 863, 113 (2018)
- G. Iorio, and V. Belokurov, *MNRAS*, 482, 3868 (2019)
- A. Helmi, C. Babusiaux, H.H. Koppelman et al., *Nature*, 563, 85 (2018)
- D. Horta, R.P. Schiavon, J. Ted Mackereth, et al. *MNRAS*, 493, 3363 (2020)
- R.A. Ibata, G. Gilmore, and M.J. Irwin, *Nature*, 370, 194 (1994)
- T.D. Kinman, and W.R. Brown, *AJ*, 141, 168 (2011)
- L. Lindegren, J. Hernandez, A. Bombrun et al., *A&A*, 616, A2 (2018)
- S.R. Majewski, M.F. Skrutskie, M.D. Weinberg, J.C. Ostheimer, *ApJ*, 599, 1082 (2003)
- S.R. Majewski, R.P. Schiavon, P.M. Frinchaboy et al., *AJ*, 154, 94 (2017)
- N. Mandelker, A. Dekel, D. Ceverino, et al., *MNRAS*, 443, 3675 (2014)
- E. Moreno, B. Pichardo, W.J. Schuster, *MNRAS*, 451, 705 (2015)
- G.C. Myeong, N.W. Evans, V. Belokurov, J.L. Sanders, and S.E. Koposov, *ApJL*, 856, L26 (2018)
- G.C. Myeong, E. Vasiliev, G. Iorio, N.W. Evans, and V. Belokurov, *MNRAS*, 488, 1235 (2019)
- P.J. McMillan, *MNRAS*, 465, 76 (2017)
- P.J. McMillan, *MNRAS*, 414, 2446 (2011)
- R.P. Naidu, C. Conroy, A. Bonaca et al. *ApJ*, 901, 48 (2020)
- P.E. Nissen, and W.J. Schuster, *A&A*, 511, L10 (2010)
- A.B.A. Queiroz, C. Chiappini, A. Perez-Villegas et al., *A&A*, 638, A76 (2020)
- R. Schonrich, J. Binney, and W. Dehnen, *MNRAS*, 403, 1829 (2010)
- W.J. Schuster, J.G. Fernández-Trincado, and E. Moreno, *IAUS*, 344, 134 (2019)
- B. Sesar, N. Hernitschek, S. Mitrovic et al., *AJ*, 153, 204 (2017)
- V.V. Smith, et al., in preparation (2020)
- Y.-S. Ting, C. Conroy, H.-W. Rix, and P. Cargile, *ApJ*, 879, 69 (2019)
- L.L. Watkins, N.W. Evans, V. Belokurov et al., *MNRAS*, 398, 1757 (2009)
- M.-S. Xiang, Y.-S. Ting, H.-W. Rix et al., *ApJS*, 245, 34 (2019)
- G. Zasowski, M. Schultheis, S. Hasselquist et al., *ApJ*, 870, 138 (2019)
- H. Zhan, *Scientia Sinica Physica, Mechanica & Astronomica*, 41, 1441 (2011)
- G. Zhao, Y.Q. Chen, J.R. Shi et al., *Chinese Journal of Astronomy and Astrophysics*, 6, 265 (2006)
- G. Zhao, Y.H. Zhao, Y.Q. Chu, Y.P. Jing, L.C. Deng, *Research in Astronomy and Astrophysics*, 12, 723 (2012)